Physics Letters A 183 (1993) 441–445
North-Holland

PHYSICS LETTERS A

Loop-cluster algorithm: an application for the 2D quantum Heisenberg antiferromagnet

He-Ping Ying [a], U.-J. Wiese [b] and Da-Ren Ji [a]

[a] *Zhejiang Institute of Modern Physics, Zhejiang University, Hangzhou 310027, China*
[b] *HLRZ, c/o KFA Jülich, P.O. Box 1913, 5170 Jülich, Germany*

Received 24 June 1993; revised manuscript received 15 October 1993; accepted for publication 19 October 1993
Communicated by J. Flouquet

A new type of cluster algorithm that strongly reduces the critical slowing down and frustration effects is developed to simulate the spin *one half* quantum Heisenberg antiferromagnet. The numerical results for the 2D system show that the method can be applied to study efficiently quantum spin systems at lower temperatures with large *Trotter* number.

The discovery of high-T_c superconductivity [1] has brought about a renewed interest in two-dimensional (2D) quantum systems such as the Hubbard model [2] and the $s=\frac{1}{2}$ Heisenberg antiferromagnet [3]. Experimentally, the first-T_c superconductor discovered was $La_{2-x}Ba_xCuO_4$ with $x\approx 0.15$ [1]. This material has a layered structure with 2D copper–oxygen planes and the quantum spin-fluid behavior was observed in undoped mother materials [4]. Theoretically, a pairing mechanism, mediated by spin fluctuations, was proposed to explain high-T_c superconductivity [5]. Both mechanisms indicate that spin dynamics plays a crucial role in the new superconducting mechanism, which is believed to originate from the purely electronic degrees of freedom. As a first stage to understand the physics of the superconductors it is already a nontrivial problem to understand insulators, their precursor, and in most cases it is difficult to find a complete analytic solution. Therefore it is natural to use a numerical approach to study the properties of these superconducting materials. In ref. [3], Barnes reviewed the different numerical methods and their results in studies of the $s=\frac{1}{2}$ quantum Heisenberg antiferromagnet (QHAF). One of the important techniques described for the calculation of the partition function is the Suzuki–Trotter (ST) approach [6]. The main idea of the ST algorithm is that the partition function of a d-dimensional quantum spin system at finite temperature and finite volume is expressed as a path integral equivalent to a $(d+1)$-dimensional classical system of Ising-like spin variables with four-spin couplings. The induced classical spin system is then simulated on a Euclidean space–time lattice using the *importance sampling* technique. Since the pioneering work of Suzuki and co-workers [6], Monte Carlo (MC) simulation has played an important role in such studies [7–11].

There are, however, some difficulties with the standard MC estimates using the importance sampling technique for the induced classical systems with multi-spin interactions [7,8,12]. Last year, a cluster algorithm was proposed for the 1D quantum Heisenberg antiferromagnet using a blockspin scheme [12] to resolve the problems related to the conservation law in quantum systems. The results showed that the blockspin cluster algorithm could update efficiently the spin configurations of 2D induced classical spin systems by avoiding the appearance of forbidden configurations and slowing down effects, both at low temperatures and in the continuum limit, i.e. $\epsilon\to 0$, where ϵ is the lattice spacing in the Euclidean time direction). For the 2D quantum spin systems, however, the algorithm meets severe problems because of the frustration effect.

Recently, a loop-cluster algorithm for the vertex model, equivalent to the $s=\frac{1}{2}$ quantum Heisenberg chain, has been proposed by Evertz and Marcu [13]. Their algorithm constructs closed loops of spins and flips them

0375-9601/93/$ 06.00 © 1993 Elsevier Science Publishers B.V. All rights reserved.

simultaneously. In this paper, we develop the Evertz–Marcu algorithm for the 2D QAFH and find that it does not suffer from the frustration and the so-called freezing effect. The calculations of the dynamical exponents of the internal energy e, and the uniform and staggered susceptibilities, χ and χ_s, respectively, show that the collective update approach can simulate the system more efficiently than other algorithms by using a much larger Trotter number m. We have also made some estimates of these thermodynamic quantities using improved estimators [14].

The spin system of 2D QHAF is described by the following Hamiltonian defined on a square $L\times L$ lattice, with periodic boundary conditions,

$$H=J\sum_{\langle i,j\rangle}\boldsymbol{S}_i\cdot\boldsymbol{S}_j=J\sum_{\langle i,j\rangle}H_{i,j}\,,\qquad \text{for } J>0\,, \tag{1}$$

where $i=(x, y)$ denotes a lattice site and $\langle i, j\rangle$ the sum over all nearest-neighbor pairs on the 2D lattice. The quantities $\boldsymbol{S}=\frac{1}{2}\boldsymbol{\sigma}$ are spin operators defined on each lattice site i (where the components of $\boldsymbol{\sigma}$ are Pauli spin matrices). By the checkerboard decomposition, $H=H_1+H_2+H_3+H_4$, with

$$H_1=J\sum_{(2k-1,l)}H_{i,i+\hat{x}}\,,\qquad H_2=J\sum_{(k,2l-1)}H_{i,i+\hat{y}}\,,\qquad H_3=J\sum_{(2k,l)}H_{i,i+\hat{x}}\,,\qquad H_4=J\sum_{(k,2l)}H_{i,i+\hat{y}}\,, \tag{2}$$

we can use the Suzuki–Trotter formula [6,7] for the partition function of eq. (1). Thus,

$$Z=\mathrm{Tr}[\exp(-\beta H)]=\lim_{m\to\infty}\mathrm{Tr}[\exp(-\epsilon H_1)\exp(-\epsilon H_2)\exp(-\epsilon H_3)\exp(-\epsilon H_4)]^m\,, \tag{3}$$

where $\hat{x}$ ($\hat{y}$) is the unit vector in the x (y) direction, $\beta=1/T$ the reduced inverse temperature and $\epsilon=\beta/m$ determines the lattice spacing in the Euclidean time direction. After inserting the complete sets of eigenstates $|+1\rangle$ and $|-1\rangle$ of σ^z between the factors of $\exp(-\epsilon H_i)$, we map the 2D quantum system to a 3D induced classical system of Ising-like variables $s(x, y, t)=\pm 1$. Explicitly we have

$$Z=\mathrm{Tr}[\exp(-\beta H)]=\prod_{(x,y,t)}\sum_{s(x,y,t)=\pm 1}\exp[-S(\{s(x,y,t)\})]\,. \tag{4}$$

In eq. (4), $S(\{s(x, y, t)\})$ denotes the four-spin interactions associated with the time-like plaquettes (see the corresponding figures in ref. [12]) and is given by the product of the transfer matrices in the σ^z representation for a given configuration $C_i=(s_1, s_2, s_3, s_4)$. That is,

$$\exp(-S[s_1,s_2,s_3,s_4])=\langle s_1,s_2|\exp(-\tfrac{1}{4}\epsilon J(\boldsymbol{\sigma}_i\cdot\boldsymbol{\sigma}_j)|s_3,s_4\rangle$$

$$=\exp(-\tfrac{1}{4}\epsilon J)\begin{pmatrix}1 & 0 & 0 & 0\\ 0 & \frac{1}{2}[\exp(\epsilon J)+1] & \frac{1}{2}[\exp(\epsilon J)-1] & 0\\ 0 & \frac{1}{2}[\exp(\epsilon J)-1] & \frac{1}{2}[\exp(\epsilon J)+1] & 0\\ 0 & 0 & 0 & 1\end{pmatrix}. \tag{5}$$

As can be seen, most spin configurations are forbidden because the corresponding elements of the transition matrices are zero ($S[s_1, s_2, s_3, s_4]=\infty$). This causes problems in numerical simulations. In a previous paper [12], a blockspin scheme was introduced to resolve the constraints and critical slowing down was eliminated for the one-dimensional QHAF. For the 2D case, on the other hand, frustration causes problems for the blockspin cluster algorithm and therefore we introduce the following loop-cluster algorithm [13] for Monte Carlo updates.

The algorithm constructs loops by first selecting a starting point (x, y, t) at random. The spin $s(x, y, t)$ participates in two plaquette interactions, one at a Euclidean time less than t and the other at a Euclidean time larger than t. When $s(x, y, t)=1$, we consider the plaquette interaction at the later time slice, while for $s(x, y, t)=-1$, we consider the interaction at the earlier time slice. The corresponding plaquette configuration is characterized by the spin orientations at the four corners of the plaquette, one of which will be the next point

of the loop. This is, the direction of growing a bond belongs to one of the space-like, time-like or diagonal directions. For configurations $C_1=[1, 1, 1, 1]$ and $C_1'=[-1, -1, -1, -1]$, the next point of the loop is the time-like nearest neighbor of (x, y, t) on the interaction plaquette. For $C_2=[1, -1, 1, -1]$ and $C_2'=[-1, 1, -1, 1]$ the next point is, with $p=2/[1+\exp(\epsilon J)]$, the time-like nearest-neighbor or, with $1-p$, the space-like nearest-neighbor of (x, y, t). For configurations $C_3=[1, -1, -1, 1]$ and $C_3'=[-1, 1, 1, -1]$, the next point is the space-like nearest-neighbor of (x, y, t). Once the next point on the loop is determined the process is repeated until the loop closes. The above probability is determined in such a way that the algorithm obeys the detailed balance $P(C_i)W(C_i\to C_j)=P(C_j)W(C_j\to C_i)$, where the configuration weights are

$$P(C_1)=P(C_1')=1\,,\qquad P(C_2)=P(C_2')=\tfrac{1}{2}[\exp(\epsilon J)+1]\,,\qquad P(C_3)=P(C_3')=\tfrac{1}{2}[\exp(\epsilon J)-1] \tag{6}$$

(see also eq. (5)) and $W(C_i\to C_j)$ is the transition probability to go from a configuration C_i to C_j. A Monte Carlo sweep is defined by constructing the loop and then flipping all the spins on the loop collectively. As will be shown by our MC indication, for the induced spin systems defined on the $L\times L\times 4m$ lattices ($4m$ is chosen as large as 768 to keep $\epsilon=\beta/m<0.1$), the algorithm described above generates the allowed configurations only. In addition, it offers the possibility of using improved estimators which further reduce the statistical fluctuation for the different observables averaged by MC simulation.

To demonstrate the efficiency of the loop-cluster algorithm we first measured the autocorrelation functions $C_{\mathcal{O}}(t)$,

$$C_{\mathcal{O}}(t)=\langle\,\mathcal{O}(t_0)\,\mathcal{O}(t_0+t)\,\rangle\,, \tag{7}$$

where $\mathcal{O}$ denotes the observables (i.e., the internal energy e, the uniform and staggered susceptibilities, χ and χ_s), and then we carefully analyzed $C_{\mathcal{O}}(t)$ to obtain the integrated autocorrelation times $\tau_{\mathcal{O}}$ via

$$\exp(-1/\tau_{\mathcal{O}})=\sum_{t=1}^{\infty}\mathcal{O}(t)\Big/\sum_{t=0}^{\infty}\mathcal{O}(t)\,, \tag{8}$$

where $\tau_{\mathcal{O}}$ are measured by one-hit loop-cluster updating. Using the data obtained in such a way we can determine the dynamical critical exponent z which is defined in the continuum limit by $\tau_{\mathcal{O}}\propto 1/\epsilon^z$ for $\epsilon\to 0$. As "high" temperature superconductor transition temperatures are of the order of 100 K with $J=1540(60)$ K [15], it is clearly the low temperature properties of the system that are of interest. We are thus concerned with the characteristics in the region $\beta J\geqslant 5.0$ and find

$$\tau_e\leqslant 1.0\,,\qquad \tau_\chi\leqslant 1.0\,,\qquad \tau_{\chi_s}\leqslant 1.0\,,\qquad z_e=z_\chi=z_{\chi_s}=0.1(1)\,. \tag{9}$$

There is no indication of slowing down for $m=64$, 128, 192 which are required for low temperatures. Next, to show the efficiency of the loop-cluster algorithm, we have performed some MC estimates at several temperature points with the same lattice sizes and m values as in ref. [9]. The calculated results are listed in table

Table 1
Some estimates of e, χ_s and χ to compare with those in table 1 of ref. [9]. N_{MC} is the number of independent MC runs and N_{sweep} of sweeps used for the MC average.

T/J	$(L^2, 4m)$	N_{MC}	N_{sweep}	e		χ_s	3χ	
				present results	ref. [9]		present results	ref. [9]
2.0	$(24^2, 64)$	11	10^5	−0.2010(15)	−0.2003(3)	0.2146(4)	0.2279(5)	0.227(2)
1.0	$(32^2, 64)$	11	10^5	−0.3871(9)	−0.3885(8)	0.8012(27)	0.2804(10)	0.281(2)
0.85	$(24^2, 128)$	11	10^5	−0.4402(17)	−0.4392)	1.191(6)	0.2807(10)	0.281(2)
0.50	$(32^2, 128)$	8	2×10^4	−0.5925(25)	−0.5946(5)	7.284(56)	0.2363(30)	0.236(2)
0.25	$(32^2, 192)$	1	10^5	−0.6667(10)	−0.6669(1)	117.5(5)	0.1615(10)	0.155(7)

1, and are in perfect agreement with those given by Makvić and Ding [9], who introduced a parallel updating technique for large-scale lattice simulation. For further information on the system, some numerical calculations of e, χ and χ_s at different temperatures are shown in figs. 1–3. The initial configurations are always taken to be random and followed by 5000 sweeps for thermalization and 50000 sweeps for the MC average using the loop-cluster algorithm. The finite size results of these thermodynamic quantities ($L=8, 10, ..., 20$) at lower temperatures ($\beta J=5, 10, 15$) have been used to calculate the important low energy parameters of the system

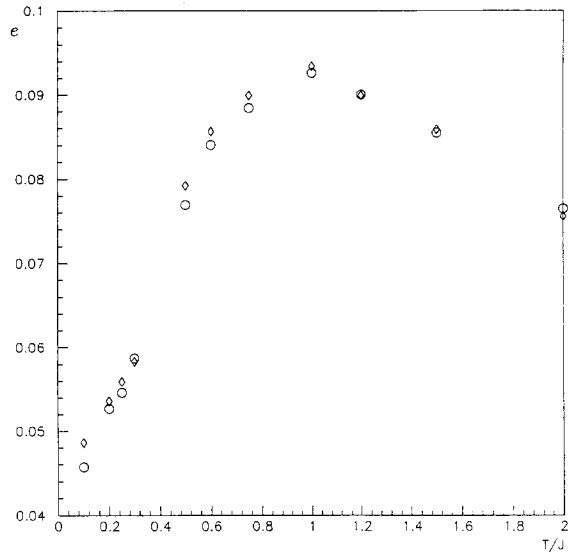

Fig. 1. Plot of the internal energy density e versus the temperature T on $L\times L$ lattices with $L=12$ (○) and 32 (◇).

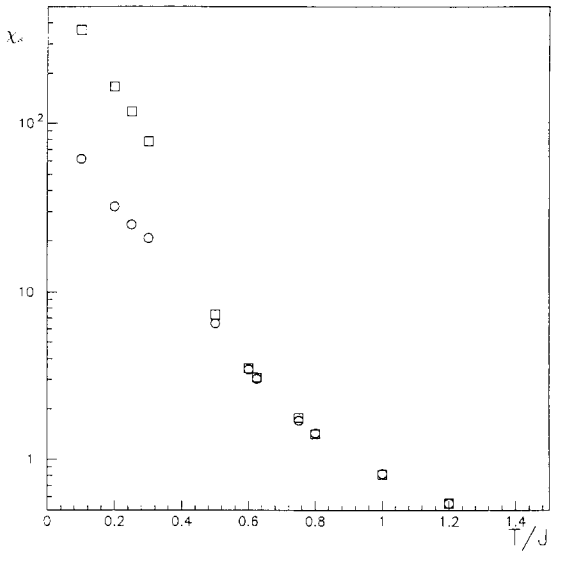

Fig. 2. Plot of the staggered susceptibility χ_s versus the temperature T on $L\times L$ lattices with $L=12$ (○) and 32 (□).

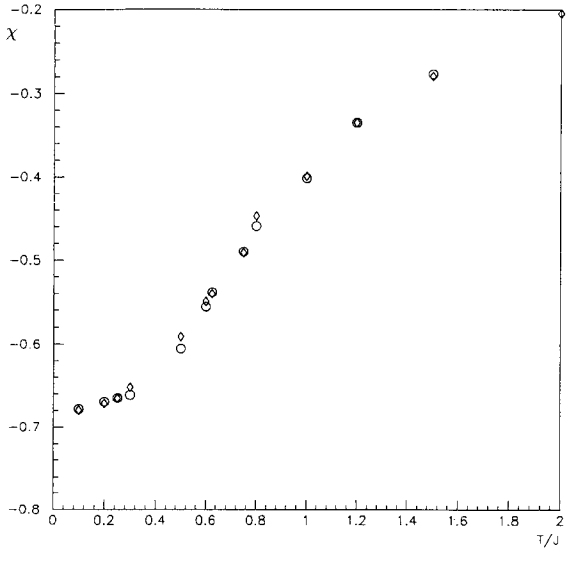

Fig. 3. Plot of the uniform susceptibility χ versus the temperature T on $L\times L$ lattices with $L=12$ (○) and 32 (◇).

[15], which determine the dynamics of the Goldstone bosons of the system using the results of chiral perturbation theory up to second loop order [16].

To summarize, we have performed a Monte Carlo measurement for 2D QAFH, using the loop-cluster algorithm, for different square $L \times L$ lattices for βJ in the range 1.0–15.0. The results for the autocorrelation times show that the algorithm can update the induced classical spin system efficiently. The study also shows that the new type of cluster method can be used to simulate the $(d+1)$-dimensional induced classical spin system at lower temperatures without suffering from slowing down effects. During the simulation for a given temperature we keep m large enough to reduce the systematic error, which is of order of $O(\epsilon^2)$. With the standard local algorithms [7–10], it would be impossible to reach temperatures as low as those we use here because of problems with slowing down effects.

We are grateful to P. Hasenfratz for useful suggestions and discussions. This work is in part supported by the National Education Commission of China. H.-P. Ying would like to thank Professor Abdus Salam, the International Atomic Energy and UNESCO for hospitality at the ICTP, Trieste.

References

[1] G. Bendorz and J.A. Müller, Z. Phys. B 64 (1986) 186;
M.K. Wu et al., Phys. Rev. Lett. 58 (1987) 908.
[2] A.P. Balachandran et al., Lecture notes in physics, Vol. 38. Hubbard model and anyon superconductivity (World Scientific, Singapore, 1990).
[3] T. Barnes, Int. J. Mod. Phys. C 2 (1991) 659.
[4] G. Shirane et al., Phys. Rev. Lett. 59 (1987) 1613.
[5] P.W. Anderson, Science 235 (1987) 1196;
T.M. Rice, Z. Phys. B 67 (1987) 141.
[6] M. Suzuki, Prog. Theor. Phys. 56 (1976) 1454; J. Stat. Phys. 43 (1986) 833;
M. Suzuki, S. Miyashita and A. Kuroda, Prog. Theor. Phys. 58 (1977) 1377.
[7] J.J. Cullen and D.P. Landau, Phys. Rev. B 27 (1983) 297.
[8] H. de Raedt and A. Lagendijk, Phys. Rep. 127 (1985) 233.
[9] H.-Q. Ding and M.S. Makivić, Phys. Rev. B 42 (1990) 6827;
M.S. Makivić and H.-Q. Ding, Phys. Rev. B 43 (1991) 3562.
[10] Y. Okabe and M. Kikuchi, J. Phys. Soc. Japan 57 (1988) 4351.
[11] J.D. Reger and A.P. Young, Phys. Rev. B 37 (1988) 5978;
J.D. Reger, J.A. Riera and A.P. Young, J. Phys. 1 (1989) 1855.
[12] U.-J. Wiese and H.-P. Ying, Phys. Lett. A 168 (1992) 143; Nucl. Phys. B Proc. Suppl. 30 (1993) 281.
[13] H.G. Evertz et al., Tallahassee preprint, FSU-SCRI-92-164;
H.G. Evertz and M. Marcu, Nucl. Phys. B, Proc. Suppl. 30 (1993) 277.
[14] U. Wolff, Phys. Rev. Lett. 62 (1989) 361; Nucl. Phys. B 334 (1990) 581.
[15] U.-J. Wiese and H.-P. Ying, Bern preprint, BUTP-92/50; accepted for publication in Z. Phys. B.
[16] P. Hasenfratz and F. Niedermayer, Bern preprint, BUTP-92/45; accepted for publication in Z. Phys. B.